

## Dynamics in hydrogen bonded liquids: water and alcohols

E. Guàrdia <sup>a</sup>, J. Martí <sup>a</sup>, J. A. Padró <sup>b</sup>, L. Saiz <sup>c</sup> and A. V. Komolkin <sup>d</sup>

<sup>a</sup> Departament de Física i Enginyeria Nuclear, Universitat Politècnica de Catalunya, Sor Eulàlia d'Anzizu s.n., B4-B5, 08034, Barcelona, Spain.

<sup>b</sup> Departament de Física Fonamental, Universitat de Barcelona, Diagonal 647, 08028 Barcelona, Spain.

<sup>c</sup> Center for Molecular Modeling, University of Pennsylvania, 231 S. 34th St., Philadelphia, PA 19104-6323, U.S.A.

<sup>d</sup> Institute of Physics, St. Petersburg State University, 198904 St. Petersburg, Russia.

Molecular dynamics (MD) has been revealed as a powerful tool to investigate the structure and dynamics of hydrogen bonded liquids. This paper reviews recent works in which MD simulations have been used to study the influence of hydrogen bonding on different dynamic properties of liquid water and alcohols. The analysed properties include intermolecular vibrations, self-diffusion coefficients and reorientational correlation times. Finally, we present a MD study of the translational and reorientational dynamics of supercooled water at pressures up to 400 MPa. The influence of hydrogen bonding on the anomalous behaviour of the dynamic properties of liquid water at high pressures and low temperatures is discussed.

### 1. INTRODUCTION

A detailed knowledge of the microscopic properties of liquids such as water and alcohols is essential for a deep understanding of many chemical and biological processes. It is well known that the properties of these liquids are markedly influenced by the existence of intermolecular hydrogen bonds. Experimental information on the microscopic properties of these systems has been obtained from X-ray and neutron diffraction, infrared and Raman spectroscopy, dielectric relaxation, etc. Since analytical theories of associated liquids cannot be easily developed, theoretical studies are frequently based on atomistic computer simulations such as molecular dynamics. Although based on effective interaction potentials, MD provides detailed pictures of atomic and molecular motions. This detailed information, which can not be obtained from other methods, is very useful for the development of new theories and models as well as for the reliable interpretation of experimental data. The main objective of the MD studies reported in this contribution is to investigate the relationship between hydrogen bonding and molecular behaviour in liquid water and alcohols. The paper is organized as follows. In Section 2 a procedure

to determine the lifetime of the H-bonds from computer simulations is described and it is applied to different alcohols including methanol, ethanol, ethylene glycol and glycerol. The results are compared with those obtained for liquid water. Section 3 is devoted to investigate the influence of the hydrogen bonds upon different single particle dynamic properties. The analysed systems are water, methanol and ethanol. Finally, in Section 4 we report preliminary results of a MD study of the dynamics and hydrogen bonding in high pressure water.

## 2. H-BOND DEFINITION, STATISTICS AND LIFETIMES

Since in MD simulations the intermolecular energy of the system is described by a continuous interaction potential we cannot distinguish with precision whether two molecules are H-bonded or not. Consequently, the adoption of a criterion to decide that one H-bond is established, is somewhat arbitrary. The H-bond definitions commonly used are based either in energetic or geometric criteria [1,2]. In our studies [3–7], we adopted a geometric definition, i.e. we assumed that a H-bond exists between two oxygens of two different molecules if three conditions are fulfilled:

1. The distance  $R_{OO}$  between the oxygens is smaller than  $R_{OO}^c$ ,
2. The distance  $R_{OH}$  between the "acceptor" oxygen and the hydrogen corresponding to the molecule of the "donor" oxygen is smaller than  $R_{OH}^c$ , and
3. The H-O...O angle is smaller than  $\varphi^c$ .

As cut-off distances  $R_{OO}^c$  and  $R_{OH}^c$  we selected the position of the first minimum of the radial distribution functions  $g_{OO}(r)$  and  $g_{OH}(r)$ , respectively. As in other studies [8] we have chosen  $\varphi^c = 30^\circ$  since the number of pairs of oxygens which satisfying conditions 1 and 2 form an angle  $\varphi > 30^\circ$  is almost negligible for all the simulated systems. One of the advantages of the use of the geometrical definition is that we can identify which hydrogen and oxygen atoms participate in each H-bond. Hence, in a given configuration, we can classify the hydrogen and oxygen atoms of the different molecules according to the total number of H-bonds in which they participate. Therefore, we can calculate separately the properties of atoms and molecules with different H-bonding states.

The procedure described above was applied to study the hydrogen bonded network of different alcohols and water at room conditions [3]. The results are summarized in Tables 1 and 2, where  $f_n^H$ ,  $f_n^O$  and  $f_n$  are the percentages of hydrogens (of the OH groups), oxygens and molecules with  $n$  ( $n = 0, 1, 2, 3, \dots$ ) H-bonds and  $n_{HB}$  is the mean number of H-bonds per molecule. The majority of molecules in liquid methanol and ethanol have 2 H-bonds which indicates that their structure is basically constituted by linear chains of H-bonded molecules (in these systems, with one hydroxyl group per molecule,  $f_n^O = f_n$ ). Molecules with 1 H-bond are at the end of the chains whereas those with 3 H-bonds should be associated with branching. The situation is very different for ethylene glycol and glycerol. For these systems, the largest part of oxygens have also 2 H-bonds but the differences between  $f_2^O$ ,  $f_1^O$  and  $f_3^O$  are smaller than for methanol and ethanol. We observe that  $f_2^O$  diminishes, while  $f_1^O$  and  $f_3^O$  increase, as the number of hydroxyl groups per molecule increases. Moreover, oxygen atoms with  $n=2$  in ethylene glycol and glycerol

Table 1

Percentages of oxygens and hydrogens with  $n$  H-bonds for different alcohols and water at room conditions [3].

System	$f_0^O$	$f_1^O$	$f_2^O$	$f_3^O$	$f_4^O$	$f_5^O$	$f_0^H$	$f_1^H$
methanol	1	16.5	75.5	7	0	0	6.0	94.0
ethanol	1	13	81	5	0	0	5.5	94.5
ethylene glycol	1	18	67	13.5	0.5	0	5.5	94.5
glycerol	2.5	24	58	15	0.5	0	9.5	90.5
water	0	2	13.5	37.5	42	5	11.5	88.5

Table 2

Percentages of molecules with  $n$  H-bonds and mean number of H-bonds per molecule for different alcohols and water at room conditions [3].

System	$f_0$	$f_1$	$f_2$	$f_3$	$f_4$	$f_5$	$f_6$	$f_7$	$f_8$	$f_9$	$n_{HB}$
methanol	1	16.5	75.5	7	0	0	0	0	0	0	1.9
ethanol	1	13	81	5	0	0	0	0	0	0	1.9
ethylene glycol	0	0	3.5	24	55.5	15	2	0	0	0	3.9
glycerol	0	0	0.5	2.5	12.5	30	34.5	16	3.5	5	5.7
water	0	2	13.5	37.5	42	5	0	0	0	0	3.3

molecules should be associated with branching. Results in Table 2 show that branching is very important in liquid ethylene glycol and glycerol. The percentage of ethylene glycol molecules with 2 H-bonds is very low and it is even smaller in the case of glycerol. In both liquids,  $f_1 = 0$ . These findings show that, unlike in alcohols with one hydroxyl group, there are no linear H-bonded chains in ethylene glycol and glycerol. Despite these differences the mean number of H-bonds per oxygen atom is very close ( $\simeq 1.9$ ) for the four alcohols and  $n_{HB}$  is proportional to the number of OH groups per molecule. Results for water are very different from those for alcohols. It could be expected some similarity between the structure of water and that of ethylene glycol because in both cases the molecules have two hydrogen atoms which may participate in H-bonds. Although for both water and ethylene glycol the majority of molecules have 4 H-bonds, the percentages for other  $n$ -values are markedly different. The percentage of non H-bonded hydroxyl hydrogens is similar for methanol, ethanol and ethylene glycol whereas for glycerol is somewhat higher and closer to that for water.

The study of the temporal evolution of the H-bonds is complicated because of the fast intermolecular vibrational motions which rearrange the H-bonds patterns producing the breaking and subsequent reformation of H-bonds in short intervals of time. We obtained the survival probability or lifetime of the H-bonds from the long time decay of the autocorrelation functions

$$C_{HB}(t) = \frac{\langle \eta_{ij}(t) \cdot \eta_{ij}(0) \rangle}{\langle \eta_{ij}(0)^2 \rangle} \cong \exp \left\{ -\frac{t}{\tau_{HB}} \right\} \quad (\text{at long times}) \quad (1)$$

Table 3

Lifetime of the H-bonds and molecular dipole moment reorientational times for different alcohols and water at room conditions [3].

System	$\tau_{HB}^C$ (ps)	$\tau_{HB}^R$ (ps)	$\tau_{HB}^I$ (ps)	$\tau_\mu$ (ps)
methanol	1.5	16	16.5	10
ethanol	2.5	36	37	27
ethylene glycol	2.0	39	44	97
glycerol	3.0	110	115	450
water	0.5	2.5	3	3.2

where the variable  $\eta_{ij}(t)$  takes the values 0 or 1 depending on the H-bond state of a given pair of oxygens:

$$\eta_{ij}(t) = \begin{cases} 1, & \text{if oxygens } i \text{ and } j \text{ are H bonded at times 0 and } t \\ & \text{and the bond has not been broken} \\ & \text{for any period longer than } t^* \\ 0, & \text{otherwise} \end{cases} \quad (2)$$

This procedure is similar to that proposed by Rapaport [9] and Matsumoto and Gubbins [10]. The limiting cases  $t^* = 0$  and  $t^* = \infty$  correspond to the continuous H-bond lifetime ( $\tau_{HB}^C$ ) and the intermittent H-bond lifetime ( $\tau_{HB}^I$ ) proposed in Ref. [9]. We also considered an intermediate case ( $\tau_{HB}^R$ ) by taking a reasonable value of  $t^*$ , namely  $t^* = \tau_{HB}^C$ . Thus, the transition of  $\eta_{ij}(t)$  from 0 to 1 is restricted to those cases in which the H-bond was broken during an interval smaller than  $\tau_{HB}^C$ . The H-bond lifetimes are summarized in Table 3. The differences among  $\tau_{HB}^C$  for the different alcohols are not significant whereas  $\tau_{HB}^R$  is markedly higher than  $\tau_{HB}^C$  in all cases and increases with the size of molecules.  $\tau_{HB}^R$  is notoriously greater for glycerol than for the other alcohols which indicates the higher stability of the H-bonds in this liquid.  $\tau_{HB}^I$  is similar but slightly higher than  $\tau_{HB}^R$  for all the systems. The H-bond lifetimes for water are markedly lower than those for alcohols. This is consistent with the fact that water molecules show faster reorientational motions than alcohol molecules. The reorientational times of the molecular dipole moments for all the analysed systems are also reported in Table 3. It must be noticed that both  $\tau_{HB}^R$  and  $\tau_\mu$  increase with the size of the alcohol molecules. In all cases,  $\tau_{HB}^C$  is markedly smaller than  $\tau_\mu$ .

### 3. INFLUENCE OF HYDROGEN BONDING ON SINGLE PARTICLE DYNAMICS

#### 3.1. Power spectra

Atomic motions in liquids are frequently analysed through the power spectra  $S(\omega)$  of the velocity autocorrelation functions:

$$S(\omega) = \int_0^\infty \frac{\langle \vec{v}(t) \cdot \vec{v}(0) \rangle}{\langle v^2(0) \rangle} \cos \omega t \, dt \quad (3)$$

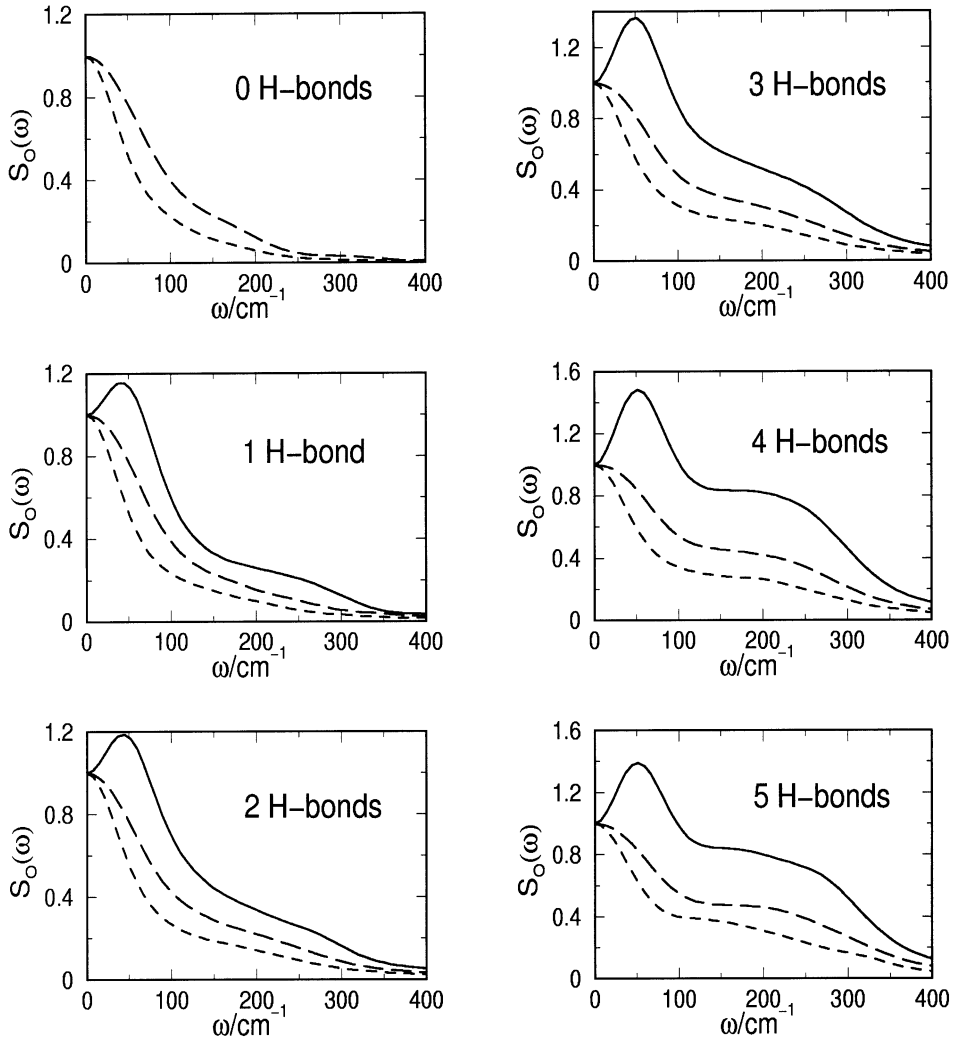


Figure 1. Normalized oxygen power spectra  $S_O(\omega)$  for water molecules with different number of H-bonds. —  $T = 298\text{ K}$ , ---  $T = 403\text{ K}$ , - - -  $T = 523\text{ K}$  [4].

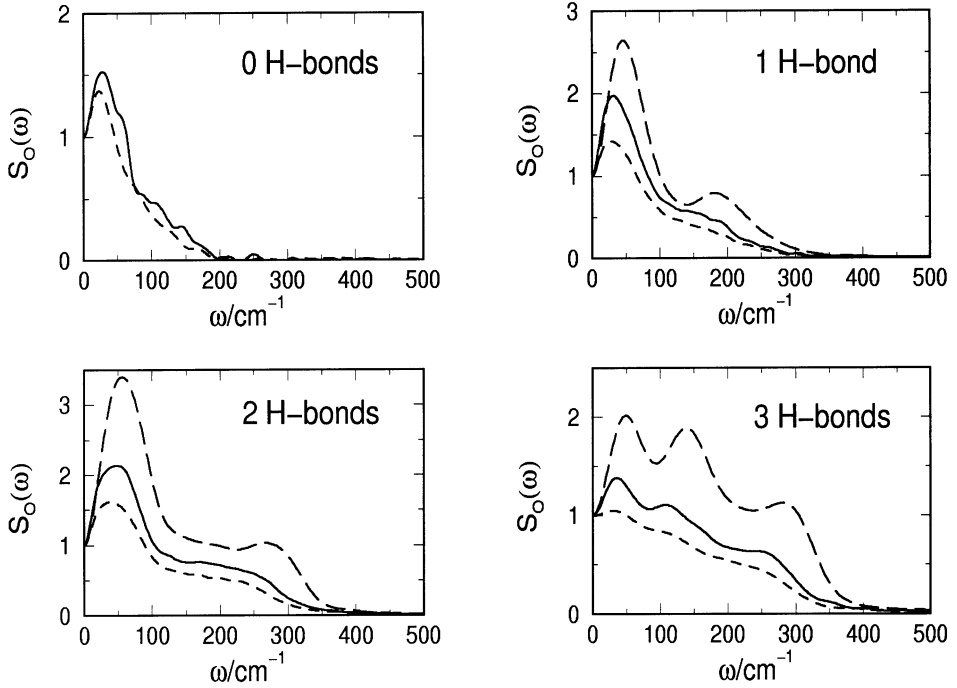


Figure 2. Normalized oxygen power spectra  $S_O(\omega)$  for methanol molecules with different number of H-bonds. --- T = 175 K , — T = 298 K , - - - T = 338 K [5].

The oxygen power spectra  $S_O(\omega)$  resulting from MD simulations of liquid water has a peak close to  $50 \text{ cm}^{-1}$  and a shoulder centered at  $200 \text{ cm}^{-1}$  which have been associated with the two bands exhibited by the Raman spectrum of this liquid in the low frequency region [11,12]. In order to investigate the physical origin of these two spectral bands we evaluated the  $S_O(\omega)$  spectra for water molecules with different numbers of H-bonds. The study was performed for different thermodynamic states along the liquid vapour coexistence curve (see Ref. [4] for more details). The resulting  $S_O(\omega)$  functions are shown in Figure 1 (at T=298 K,  $S_O(\omega)$  for water molecules with zero H-bonds cannot be calculated since the number of molecules in this H-bonding state is too low, as it can be observed from Table 1). It is interesting to note that the existence of the  $50 \text{ cm}^{-1}$  peak is independent of the H-bonding state of the molecule and depends only on the thermodynamic state of the simulated water. In contrast, the  $200 \text{ cm}^{-1}$  shoulder is more marked when the number of H-bonds increases. Similar findings are obtained when analysing the oxygen power spectra of liquid methanol and ethanol, as can be seen

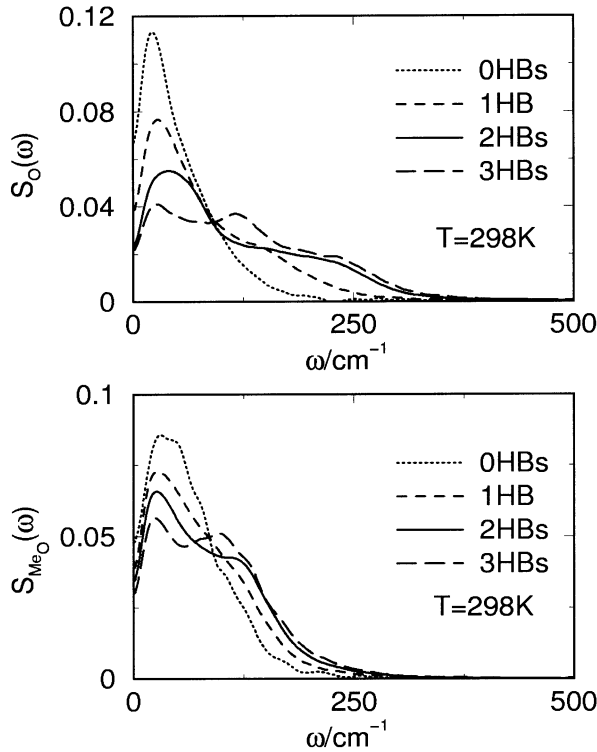


Figure 3. Power spectra corresponding to the oxygen atoms (top) and  $Me_O$  groups (bottom) for ethanol molecules with different number of H-bonds [6].

in Figures 2 and 3, respectively. In the case of methanol, a "solid" like power spectra with additional marked peaks for molecules with 3 H-bonds may be observed at  $T=175\text{K}$ . The existence of a three peak structure has been also observed in a recent instantaneous normal mode analysis of methanol at low temperature [13]. In the case of ethanol, we also analysed the power spectra corresponding to the methyl group close to the oxygen atom which was termed as  $Me_O$ . The  $S_{MeO}(\omega)$  functions resulting for molecules with different number of H-bonds are depicted in Figure 3 and they indicate that although the  $Me_O$  group has no direct participation in the H-bonds, its motion is strongly dependent on the H-bonding state of the molecule.

The results of Figures 1, 2 and 3 show that, according to the common interpretation of the experimental spectra, the shoulder of  $S_O(\omega)$  at intermediate frequencies should be associated with intermolecular motions of H-bonded molecules. However, unlike in

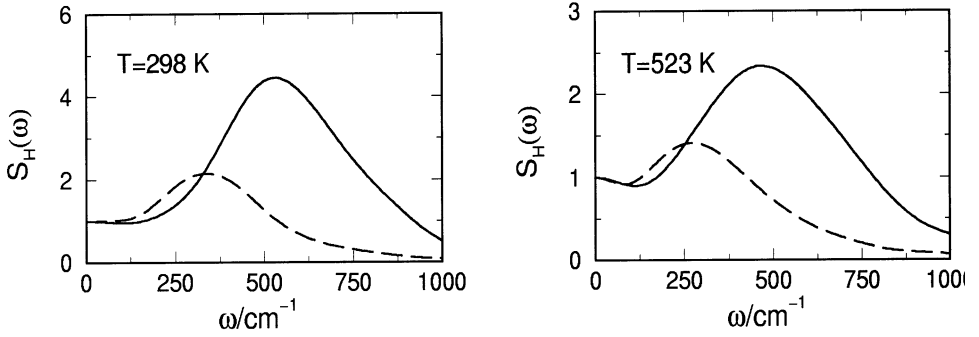


Figure 4. Normalized power spectra  $S_H(\omega)$  corresponding to H-bonded (—) and non H-bonded (---) hydrogen atoms of water molecules at  $T=298\text{ K}$  (left) and  $T=523\text{ K}$  (right) [4].

frequent interpretations of the experiments, the low frequency peak of  $S_O(\omega)$  resulting from MD simulations has no relation with the H-bonds and may be simply due to cage vibrations also present in non H-bonded liquids. Similar conclusions were obtained in a recent MD simulation study of A. Idrissi and coworkers [12] by analysing different dynamical properties. A detailed analysis of the contribution to  $S_O(\omega)$  of different kinds of intermolecular motions can be found in the MD study of water triplets performed by Stutmann and Vallauri [15].

In the case of liquid water, the hydrogen power spectra  $S_H(\omega)$  has a band at frequencies between 400 and 1200  $\text{cm}^{-1}$  which has been associated with librational modes [14]. In order to analyse the influence of hydrogen bonding on this spectral band we computed the  $S_H(\omega)$  spectra for H-bonded and non H-bonded atoms separately. As can be seen from Figure 4, H-bonds produce a marked shift of the librational band to higher frequencies. At room temperature, we observe a frequency shift of approximately 250  $\text{cm}^{-1}$ . The frequency shift slightly increases as temperature increases. A frequency shift of approximately 260  $\text{cm}^{-1}$  was observed for liquid ethanol at room conditions (see Figure 5).

### 3.2. Self-diffusion coefficients

To investigate the influence of hydrogen bonding on the mobility of the molecules we calculated the self-diffusion coefficients  $D$  for molecules with different H-bonding states. The analysis was carried out for liquid water and methanol at the same thermodynamic states as in Section 3.1. The  $D$  coefficients were calculated by integration of the oxygen velocity autocorrelation functions according to the following expression

$$D = \frac{1}{3} \int_0^\infty \langle \vec{v}(t) \cdot \vec{v}(0) \rangle dt \quad (4)$$



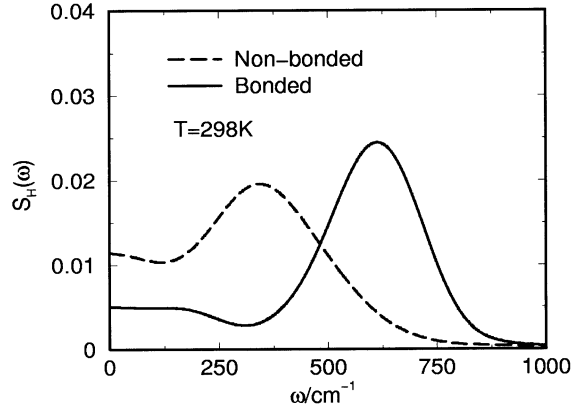


Figure 5. Power spectra corresponding to H-bonded (—) and non H-bonded (---) hydrogen atoms of ethanol molecules at room conditions [6].

In Table 4 we collect the resulting self-diffusion coefficients  $D^{(n)}$  for water and methanol molecules as a function of the number  $n$  of H-bonds in which they participate. In the case of methanol, the values corresponding to  $T=175$  K are not reported because they are too small to be accurately determined. For both liquids, the self-diffusion coefficients of the non H-bonded molecules are markedly bigger than those of the H-bonded molecules and  $D^{(n)}$  systematically diminishes as  $n$  increases. On the other hand, the  $D$  coefficients corresponding to all the molecules in the system are in good agreement with the available experimental data.

Table 4

Self-Diffusion coefficients (in  $10^{-9}$  m<sup>2</sup>/s) for water [4] and methanol [5] molecules with different number of H-bonds and averaged values.

System	Temperature	$D^{(0)}$	$D^{(1)}$	$D^{(2)}$	$D^{(3)}$	$D^{(4)}$	$D^{(5)}$	$D$	$D_{exp}$
water	298 K	—	5.7	4.4	3.2	2.2	2.0	2.6	2.3 <sup>a</sup>
	403 K	16.6	13.7	12.6	10.2	8.6	8.1	9.9	
	523 K	34.5	30.0	25.7	22.2	19.5	17.4	24.1	28.0 <sup>b</sup>
methanol	298 K	6.6	3.6	2.4	2.2	—	—	2.6	2.4 <sup>c</sup>
	338 K	9.1	6.4	4.4	3.9	—	—	4.7	4.5 <sup>c</sup>

<sup>a</sup> from Ref. [16], <sup>b</sup> from Ref. [17], <sup>c</sup> from Ref. [18]

Table 5

Reorientational correlation times (in ps) for ethanol molecules with different number of H-bonds and averaged values [7].

Temperature	$\tau_{\mu}^{(0)}$	$\tau_{\mu}^{(1)}$	$\tau_{\mu,C}^{(1)}$	$\tau_{\mu}^{(2)}$	$\tau_{\mu,C}^{(2)}$	$\tau_{\mu}^{(3)}$	$\tau_{\mu,C}^{(3)}$	$\tau_{\mu}$
223 K	—	16	13	85	110	53	350	75
298 K	6	11	6	22	45	17	35	19.5
348 K	6	7	4	9.5	19	9	—	9

### 3.3. Reorientational correlation times

Dielectric properties of polar liquids are strongly related to the reorientational motions of the molecular dipole moments (see for instance Ref. [19]). A quantitative estimation of the reorientational times can be obtained from MD simulations from the long time decay of the autocorrelation function

$$R_{\mu}(t) = \langle \hat{\mu}(t) \cdot \hat{\mu}(0) \rangle \cong \exp \left\{ -\frac{t}{\tau_{\mu}} \right\} \quad (\text{at long times}) \quad (5)$$

where  $\hat{\mu}(t)$  is a unit vector along the molecular dipole moment. In Table 5 we summarize the  $\tau_{\mu}$  values resulting for liquid ethanol at different temperatures [7]. It is natural to expect that the reorientational motions of a given molecule will depend on the number of H-bonds in which it participates. In order to analyse this dependence we determined the functions  $R_{\mu}^{(n)}(t)$  corresponding to the molecules that for a given configuration ( $t = 0$ ) have the same number  $n$  of H-bonds. The corresponding decay times  $\tau_{\mu}^{(n)}$  are also given in Table 5. As could be expected, for a given hydrogen bonding state  $\tau_{\mu}^{(n)}$  increases as temperature diminishes.

Results in Table 5 corroborate that molecular reorientations are strongly dependent on the hydrogen bonding state of the molecule. The averaged  $\tau_{\mu}$  values corresponding to all the molecules in the system are intermediate between  $\tau_{\mu}^{(1)}$  and  $\tau_{\mu}^{(2)}$  but closer to the second, which is in accordance with the fact that the majority of ethanol molecules have 2 H-bonds (see Table 2). In general,  $\tau_{\mu}^{(n)}$  increases as  $n$  increases. However there is a deviation from this rule. At  $T = 223$  K we find  $\tau_{\mu}^{(3)} < \tau_{\mu}^{(2)}$ , which should be attributed to the fact that the  $\tau_{\mu}^{(3)}$  value is much larger than the lifetime of molecules in the  $n = 3$  state. For this reason, we also determined the reorientational correlation functions  $R_{\mu,C}^{(n)}(t)$  corresponding to the molecules that remain in the initial hydrogen bonding state during the whole time interval  $t$ . This approach is equivalent to the continuous H-bond definition given in Section 2. As can be seen from Table 5, in all cases  $\tau_{\mu,C}^{(n)}$  increases as  $n$  increases. On the other hand, we get  $\tau_{\mu,C}^{(1)} < \tau_{\mu}^{(1)}$ ,  $\tau_{\mu,C}^{(2)} > \tau_{\mu}^{(2)}$  and  $\tau_{\mu,C}^{(3)} > \tau_{\mu}^{(3)}$ . This may be due to the fact that the lifetime of the  $n=2$  state is much larger than the lifetimes of the  $n=1$  and  $n=3$  states [7].

It is interesting to analyse in detail the behaviour of the  $R_{\mu,C}^{(1)}(t)$  functions for very short times (see Figure 6). After a fast initial inertial decay these functions show an oscillation which may be associated with the molecular vibrations of the COH plane around the COH bond [7]. As observed in Figure 6, the characteristic time of these librational motions for molecules whose oxygen acts as a proton acceptor is approximately two times larger than

for molecules whose oxygen acts as a proton donor. Another difference between the  $R_{\mu,C}^{(1)}(t)$  functions for molecules whose oxygen acts as proton donor and those for molecules whose oxygen acts as proton acceptor is that the relaxation of the former after the librational oscillation ( $t > 0.2$  ps) is much faster than that of the latter (see Figure 6).

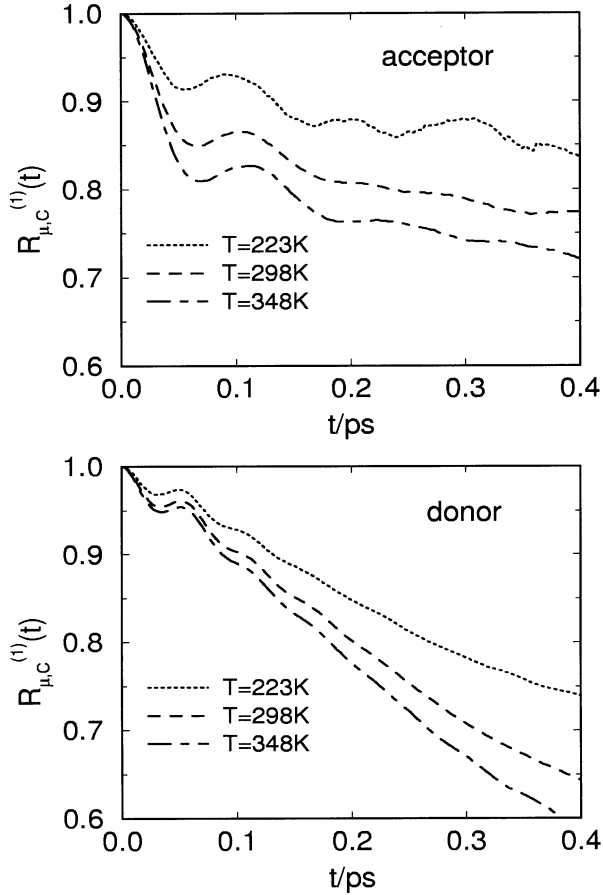


Figure 6. Short time behaviour of the reorientational correlation functions  $R_{\mu,C}^{(1)}(t)$  for ethanol molecules participating in one single hydrogen bond as acceptor (top) and donor (bottom) [7].

Table 6

Self-Diffusion coefficients ( $D$  in  $10^{-9}$  m<sup>2</sup>/s) and reorientational correlation times ( $\tau_\alpha$  in ps) for water at high pressure.

Temperature	Pressure	$D$	$D_{exp}$ [20]	$\tau_\mu$	$\tau_{HH}$	$\tau_\perp$	$\tau_{exp}$ [21]
248 K	0.1 MPa	0.5	0.31	21.1	22.0	14.9	21.4
	200 MPa	0.7	0.47	14.3	14.0	9.6	10.9
	400 MPa	0.6	0.39	13.3	13.0	9.0	
298 K	0.1 MPa	2.3	2.35	5.5	4.9	3.5	2.7
	200 MPa	2.4	2.26	4.9	4.6	3.0	2.1
	400 MPa	2.3		4.0	4.2	2.7	
348 K	0.1 MPa	5.3		2.5	2.1	1.5	1.0
	200 MPa	5.1		2.3	1.9	1.5	0.8
	400 MPa	4.6		2.0	1.9	1.4	

#### 4. DYNAMICS AND HYDROGEN BONDING IN HIGH PRESSURE WATER

The normal behaviour for liquids is to decrease their diffusivity with application of pressure. This is not the case of water at temperatures below  $T = 298$  K [20]. On the other hand, the rotational correlation times resulting from NMR experiments on water and heavy water indicate that reorientational motions become faster as pressure increases [21]. It should be interesting to know whether or not these experimental findings can be reproduced by MD simulation and to investigate their microscopic origin. In particular, it should be interesting to analyse the influence of pressure on the hydrogen bonded network of liquid water. To this end, we carried out a series of MD simulations of liquid water at different pressures and temperatures. We assumed the SPC/E water model [22]. Other technical details will be published elsewhere [23].

The self-diffusion coefficients and reorientational correlation times resulting from the different simulated systems are collected in Table 6. The  $D$  coefficients were obtained from the long time slope of the molecular mean square displacement of water molecules by using the Einstein relation

$$D = \lim_{t \rightarrow \infty} \frac{1}{6} \langle |r(\vec{t}) - r(\vec{0})|^2 \rangle \quad (6)$$

The reorientational correlation times  $\tau_\mu$ ,  $\tau_{HH}$  and  $\tau_\perp$  were obtained from the long time decay of the reorientational correlation functions

$$R_\alpha(t) = \langle \vec{u}_\alpha(t) \cdot \vec{u}_\alpha(0) \rangle \cong \exp \left\{ -\frac{t}{\tau_\alpha} \right\} \quad (7)$$

where we considered three different  $\vec{u}_\alpha$  unit vectors: a unit vector  $\vec{u}_\mu$  along the molecular dipole moment, a unit vector  $\vec{u}_{HH}$  along the  $H - H$  direction and a unit vector  $\vec{u}_\perp$  perpendicular to the molecular plane. As pressure increases, the  $D$  coefficients resulting from MD increase in supercooled water and decrease in water at high temperature. On the contrary, the reorientational correlation times diminish as pressure increases for all the

Table 7

Percentages of oxygens ( $f_n^O$ ) and hydrogens ( $f_n^H$ ) with  $n$  H-bonds for water at high pressure.

Temperature	Pressure	$f_1^O$	$f_2^O$	$f_3^O$	$f_4^O$	$f_5^O$	$f_0^H$	$f_1^H$
248 K	0.1 MPa	0.2	3.7	23.0	67.8	5.3	6.5	93.5
	200 MPa	0.2	4.0	25.3	63.5	6.8	6.9	93.1
	400 MPa	0.2	4.0	26.1	62.1	7.5	6.9	93.1
298 K	0.1 MPa	1.1	9.6	33.9	50.2	5.1	12.9	87.1
	200 MPa	0.9	8.7	33.5	50.3	6.4	12.0	88.0
	400 MPa	0.9	8.8	33.8	49.2	7.2	11.9	88.1
348 K	0.1 MPa	3.1	17.1	39.2	36.5	4.0	19.9	80.1
	200 MPa	2.5	15.2	38.5	38.4	5.2	18.1	81.9
	400 MPa	2.1	14.1	38.0	39.6	5.9	16.9	83.1

analysed temperatures. Despite the values of  $\tau_\mu$ ,  $\tau_{HH}$  and  $\tau_\perp$  for a given thermodynamic state show noticeable differences, a similar dependence of the three different reorientational times with temperature and pressure is observed. In all cases, when increasing the temperature, the effect of pressure becomes smaller. As can be seen from Table 6, the rotational correlation times  $\tau_{exp}$  resulting from NMR experiments [21] show the same pressure and temperature dependence as  $\tau_\alpha$ . We may then conclude that the MD results obtained using the SPC/E model show an overall agreement with the experimental data. The increase of  $D$  with pressure in supercooled water was also obtained by F. W. Starr and coworkers in recent MD simulations with the SPC/E model [24]. To the best of our knowledge there are no computer simulation studies devoted to the study of the influence of pressure on the reorientational motions of water molecules.

The results concerning the influence of pressure and temperature on the hydrogen bonded network are summarized in Tables 7 and 8. At room temperature the majority of water molecules have 4 H-bonds as it corresponds to the well known tetrahedral structure of liquid water. The H-bonded network is partially destroyed as temperature increases. So, at  $T=348\text{K}$  and for a given pressure, both  $f_3^O$  and  $f_2^O$  are notoriously higher and  $f_4^O$  lower than those at room temperature. The differences between the  $f_n^O$  values at  $T=248\text{K}$  and at room temperature are in the opposite sense. The analysis of the changes of  $f_n^O$  with pressure are more interesting. In liquid water at high temperature,  $f_4^O$  increases while both  $f_3^O$  and  $f_2^O$  decrease with application of pressure, which suggests that the H-bond network tends to be reinforced. On the contrary, in supercooled water an increase of pressure tends to destroy the network. So at  $T=248\text{K}$ , the value of  $f_4^O$  diminishes while the values of both  $f_3^O$  and  $f_2^O$  increase with increasing pressure. These findings suggest that the density of supercooled water at low pressures is so high that an additional reduction of the interatomic distances cannot easily be incorporated to the tetrahedral network which is partially destroyed. At room temperature the behaviour is intermediate and  $f_2^O$ ,  $f_3^O$  and  $f_4^O$  are slightly dependent on pressure. Finally,  $f_5^O$  slightly increases with pressure at all temperatures. For the sake of completeness the percentages of H-bonded ( $f_1^H$ ) and non H-bonded ( $f_0^H$ ) hydrogen atoms are also given in Table 7.

As it can be seen from Table 8, the mean number of H-bonds per molecule  $n_{HB}$  decreases

Table 8

Mean number of H-bonds per molecule ( $n_{HB}$ ) and lifetimes ( $\tau_{HB}^C$  and  $\tau_{HB}^R$ ) of the H-bonds for water at high pressure.

Temperature	Pressure	$n_{HB}$	$\tau_{HB}^C$ (ps)	$\tau_{HB}^R$ (ps)
248 K	0.1 MPa	3.74	2.2	14.8
	200 MPa	3.73	1.9	11.2
	400 MPa	3.73	1.7	10.2
298 K	0.1 MPa	3.49	0.80	4.4
	200 MPa	3.53	0.77	3.9
	400 MPa	3.53	0.73	3.6
348 K	0.1 MPa	3.21	0.45	1.9
	200 MPa	3.29	0.45	1.8
	400 MPa	3.33	0.42	1.7

as temperature increases whereas the changes of  $n_{HB}$  with pressure for a given temperature are very small.  $n_{HB}$  at T=248K does not change significantly but shows a little decrease with pressure. On the contrary,  $n_{HB}$  at T=298K shows a slight increase with pressure which is more evident at T=348K. The effect of pressure is subtle in the sense that it does not change substantially the number of H-bonds in spite of the differences on the  $f_n^O$  values discussed above. Similar conclusions were obtained by M.C. Bellisent-Funel and L. Bosio from neutron scattering studies of heavy water [25].

In general the lifetime of the H-bonds increase as temperature diminishes (see Table 8). Although the changes with pressure of both  $\tau_C$  and  $\tau_R$  are more marked at low temperature, the same tendency is observed at all temperatures, i.e. the lifetime of the H-bonds decreases as pressure increases. This shows that an increase of pressure always produces more unstable H-bonds. On the other hand, the influence of pressure is more important for  $\tau_R$  than for  $\tau_C$ , specially in the case of supercooled water.

### Acknowledgments

This work has been supported by the Spanish "Ministerio de Ciencia y Tecnología" (BFM2000-0596-CO3 Grant) and the "Generalitat de Catalunya" (1999SGR-00146 Grant).

### REFERENCES

1. D. Bertolini, M. Cassettari, M. Ferrario, P. Grigolini and G. Salvetti, Adv. Chem. Phys. 62 (1985) 277.
2. A. Geiger and P. Mausbach, in *Hydrogen Bonded Liquids*, Vol. 329 of NATO ASI Series C, edited by J. C. Dore and J. Teixeira (Kluwer, The Netherlands, 1991), pp. 171-183, and references therein.
3. J. A. Padró, L. Saiz, and E. Guàrdia, J. Mol. Struct. 416 (1997) 243.
4. J. Martí, J. A. Padró, and E. Guàrdia, J. Chem. Phys. 105 (1996) 639.
5. J. Martí, J. A. Padró, and E. Guàrdia, J. Mol. Liq. 64 (1995) 1.
6. L. Saiz, J. A. Padró, and E. Guàrdia, J. Phys. Chem. B 101 (1997) 78.
7. L. Saiz, J. A. Padró, and E. Guàrdia, Mol. Phys. 97 (1999) 897.

8. A. Luzar and D. Chandler, J. Chem. Phys., 98 (1993) 8160; Phys. Rev. Lett., 76 (1996) 928.
9. D. C. Rapaport, Mol. Phys. 50 (1983) 1151.
10. M. Matsumoto and K. E. Gubbins, J. Chem. Phys., 93 (1990) 1981.
11. G. E. Walrafen, M. S. Hokmabadi, W. H. Yanh, Y. C. Chu, and B. Monosmith, J. Phys. Chem. 93 (1989) 2909.
12. A. Idrissi, F. Sokolić, and A. Perera, J. Chem. Phys. 112 (2000) 9479.
13. G. Garberoglio and R. Vallauri, private communication.
14. J. Martí, E. Guàrdia, and J. A. Padró, J. Chem. Phys. 101 (1994) 10883.
15. G. Sutmann and R. Vallauri, J. Phys.: Condens. Matter 10 (1998) 9231.
16. K. Krynicky, C. D. Green, and D. W. Sawyer, Faraday Discuss. Chem. Soc. 66 (1978) 199.
17. R. Hausser, G. Maier, and F. Noack, Z. Naturf. A 21 (1966) 1410.
18. M. Haughney, M. Ferrario, and I. R. MacDonald, J. Phys. Chem. 91 (1987) 4934.
19. J. Barthel, K. Bachhuber, R. Buchner, and H. Hetzenauer, Chem. Phys. Letters 165 (1990) 369.
20. E. W. Lang and H. D. Lüdemann, in *Hydrogen Bonded Liquids*, Vol. 329 of NATO ASI Series C, edited by J. C. Dore and J. Teixeira (Kluwer, The Netherlands, 1991), pp. 333-356.
21. E. W. Lang and H.D.Lüdemann, Ber. Bunsenges. Phys. Chem. 85, (1981) 603.
22. H. J. C. Berendsen, J. R. Grigera, and T. P. Straatsma, J. Phys. Chem. 91 (1987) 6269.
23. E. Guàrdia, A. V. Komolkin, and J. A. Padró, in preparation.
24. F. W. Starr, S. Harrington, F. Sciortino, and H. E. Stanley, Phys. Rev. Lett. 82 (1999) 3629.
25. M. C. Bellisent-Funel and L. Bosio, J. Chem. Phys. 102 (1995) 3727.